Steel and Composite Structures, *Vol. 20, No. 2 (2016) 431-445*
DOI: http://dx.doi.org/10.12989/scs.2016.20.2.431

Pseudo-dynamic test of the steel frame – Shear wall with prefabricated floor structure

Chun Han [1,2], Qingning Li [*1], Weishan Jiang [1], Junhong Yin [1] and Lei Yan [1]

[1] *College of Civil Engineering, Xi'an University of Architecture and Technology, Xi'an, P.R. China*
[2] *College of Civil Engineering, Xinxiang University, Xinxiang, P.R. China*

(*Received March 25, 2015, Revised October 01, 2015, Accepted October 19, 2015*)

Abstract. Seismic behavior of new composite structural system with a fabricated floor was studied. A two-bay and three-story structural model with the scale ratio of 1/4 was consequently designed. Based on the proposed model, multiple factors including energy dissipation capacity, stiffness degradation and deformation performance were analyzed through equivalent single degree of freedom pseudo-dynamic test with different earthquake levels. The results show that, structural integrity as well as the effective transmission of the horizontal force can be ensured by additional X bracing at the bottom of the rigidity of the floor without concrete topping. It is proved that the cast-in-place floor in areas with high seismic intensity can be replaced by the prefabricated floor without pouring surface layer. The results provide a reliable theoretical basis for the seismic design of the similar structural systems in engineering application.

Keywords: frame-shear wall structure; fabricated floor; pseudo-dynamic test; seismic behavior

1. Introduction

It is generally agreed that traditional housing architectural, to some extent, is not able to the requirement of higher and higher architectural features and period (Sun *et al*. 2010). Therefore, it is necessary to update current architectural construction methods and realize industrialization of residential buildings. Prefabricated building is widely applied for its high efficiency, short production period and remarkable function of saving energy and reducing consumption.

In recent years, structural systems with a fabricated steel-concrete floor as representative have been extensively applied to engineering practice; nevertheless, it is still controversial with regard to its seismic performance. Related theories and experimental studies on this subject are insufficient and far away from perfection.

Earthquakes occur in China, which makes it of great necessity to carry out further research on theoretical and experimental study on seismic performance of Hybrid structure system and promote the wide use of hybrid structure system in China (Lu *et al*. 2009).

This paper is focused on the pseudo-dynamic test and the research on the seismic performance of the three-story-two-span frame –shear wall structure with a precast floor diaphragm (Nakashima *et al*. 1992, 1995, Paquette and Bruneau 2003, Paquette and Bruneau 2006, Fan *et al*. 2007, Shi *et*

*Corresponding author, Professor, M.S., E-mail: hanpeng5085@163.com

Copyright © 2016 Techno-Press, Ltd.
 ISSN: 1229-9367 (Print), 1598-6233 (Online)

al. 2011, Chen *et al*. 2014).

The results show that, structural integrity as well as the effective transmission of the horizontal force can be ensured by additional X bracing at the bottom of the rigidity of the floor without concrete topping. It is proved that the cast-in-place floor in areas with high seismic intensity can be replaced by the prefabricated floor without pouring surface layer. The results provide a reliable theoretical basis for the seismic design of the similar structural systems in engineering application.

2. Design and instrumentation of test specimen

This test model is made after the steel frame –shear wall structure is completed and the precast floor is installed on the frame-shear. The whole structure of the steel frame-shear with a fabricated floor is formed by setting the proper connection between plates, plates and steel beams, beams and columns and the X-shaped horizontal bracing .The structure layout are shown in Figs. 1-2.

2.1 Node Design (*Zheng et al*. *2013*)

2.1.1 Connection between beams and plates

Differing from the traditional single two-way reinforcement, the new type of prestressed hollow core floor, Parallel to the direction of the prestressed, uses the anchorage of the double reinforcement are used and the high strength steel are chosen to make U-shaped ribs, one rib for each hole and beams to conduct the pouring connection and promote the ability for the prefabricated floor to bear the vertical load.

The nodes between beams and plates adopt snake bending steel and have the function of resisting shear and lift. There are two advantages for the snake bending steel. First, it can bear the horizontal shear force more than anti-shear studs. Second, the snake bending steel is continuous, which makes it possible to function without the tensile and anti-lift anchoring. Meanwhile, mechanical anchoring can be formed by putting longitudinal reinforcement on the beam together with the U-shaped ribs to pass the bending moment of vertical load. As far as the edge beams are concerned, it is also possible for the superstructure to have more bending stiffness under the horizontal load. The planar is shown in Fig. 3. The reinforcement details of the precast floor is shown in Fig. 4 and the connected nodes between plates and steel beams is shown in Fig. 5(a).

2.1.2 The connection between plates

The connection between plates relies on the alveolar of the plate side to form shear connection key to pass the horizontal shear (Ren and Naito 2012, Zhang *et al*. 2010); put the precast floor with the side bar on the plate designed ahead of time and set two pieces of cold drawing with a diameter of ϕ4 where there is a joint between two plate bars and fasten them to bear the vertical load as well as increase the bending stiffness under the horizontal load. The connected nodes between the diaphragm joints of the precast floor can be seen from Fig. 5(b).

2.1.3 Other connections

The steel beams and bracing pieces adopt the method of welded connections with steel plates stuck on the column node to reinforce while the beam wed gets reinforced by adding transverse stiffeners. As for the horizontal bracing under the plate, the joint of node plates is firmly welded with that of the beam and column and the foundation supports of the model structure are made with the steel shape, fixed with the foundation bolt by pressure beam (Fleischman *et al*. 2012).

2.2 Material properties

The steel frame uses Q235 made in China, which has the same structure with prototype structure .After the material test, the average yield is 236.1 Mpa, the average ultimate strength 350.5 MPa, the average elongation 25.43% (Li *et al*. 2014).The design strength rating of the precast concrete is C40 and that of concrete diaphragm post-cast strip is C45. During the test, several groups of test cubes are made with the concrete mixture of the same batch and the compression testing is conducted. It is concluded that the average compression strength of the late poured micro concrete is 31.21 MPa. The new precast floor uses high-strength steel with the yield strength of 1,200 MPa.

2.3 Model similarity relation

The scale ratio used in the test model is S_1 = 1/4. The stress ratio of the model added with weight S_σ is 1. The same material as prototype is used in the model with the similar construction technology and quality, so the elastic modulus S_E is 1. According to Buckingham's theory and the dimensional method, the expression of the similarity relation between the model and prototype structure is derived and then some main similarity coefficient for this test is concluded .The similar condition of model dynamic can be seen in Table 1, and the model's sectional dimension designed and produced according to the reduced scale relation is shown in Table 2.

Table 1 Model similarity relation

Physical quantities	Length	Area	Elastic modulus	Shear modulus	Mass
Similarity coefficient	1/4	1/16	1	1	1/16
Physical quantities	Time	Velocity	Acceleration	Poisson's ratio	Frequency
Similarity coefficient	1/2	1/2	1	1	2

Table 2 Specimens prototype and scaled dimensions (Units: mm)

Type	The section size of prototype	The section size of model
beam	400×200×12×12	100×68×4.5×7.5
column	320×320	80×80
Steel plate shear wall	2600×2600×6	650×650×3
square steel tube	200×160	50×4

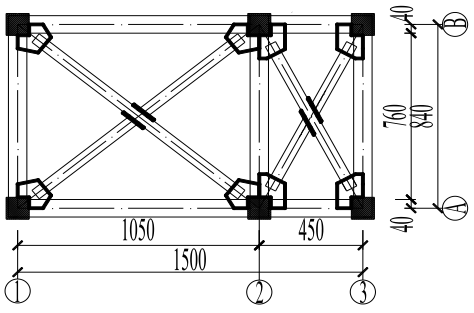

Fig. 1 Plan of structural plane layout and bottom Bracing (Units: mm)

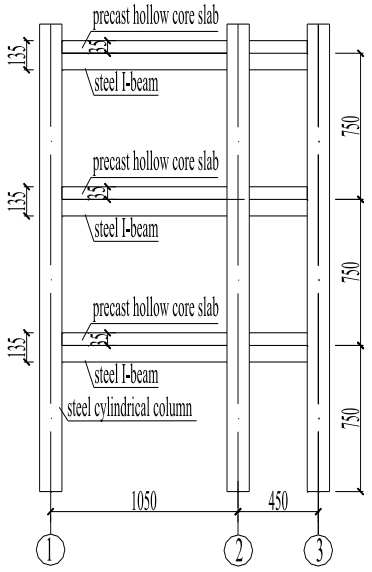

Fig. 2 Plan of structural elevation layout (Units: mm)

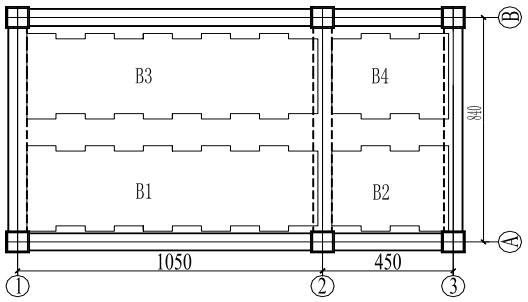

Fig. 3 Plan of structural plane layout of precast hollow core diaphragm (Units: mm)

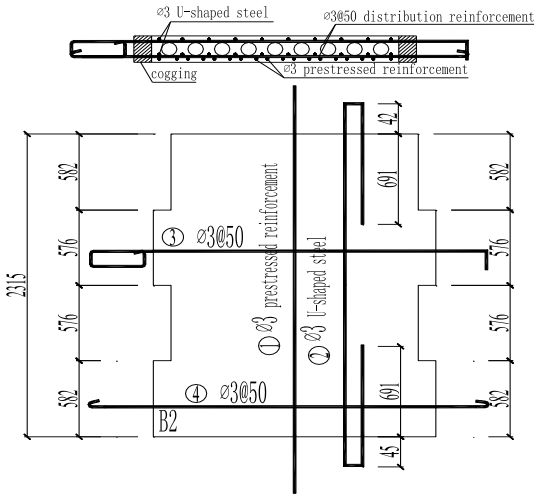

Fig. 4 B_2 reinforcement drawing of precast hollow core diaphragm (Units: mm)

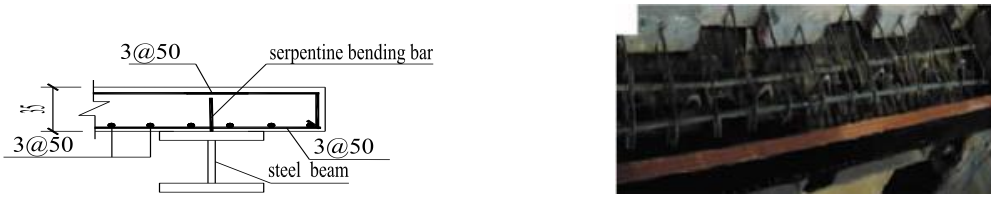

(a) Connector of plate-steel beam (Units: mm)

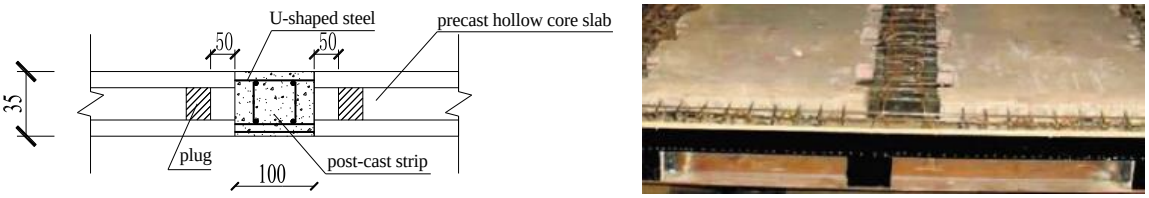

(b) Connector of precast hollow core diaphragm (Units: mm)

Fig. 5 Connector of precast assembly diaphragms (Units: mm)

2.4 Loading and testing apparatus

2.4.1 Horizontal load

The pseudo-dynamic test is conducted by the MTS electro-hydraulic servo loading system. This system is made up of L rectangular reaction wall test pedestal, servo loading system, data acquisition instrument and so on. The hydraulic servo actuator is installed on the nodal points between the bracing piece and girder of the model's third layer to apply the horizontal load, whose maximum output is +500 kN, and stroke +250 mm. The model's loading is controlled by displacement, which is calculated by analyzing the reaction of equivalent single particle system (Medhekar and Kennedy 2000, Paquette and Bruneau 2003, Priestley *et al*. 2007, Liang 2011, Chen *et al*. 2014).

2.4.2 Vertical load

In the pseudo-dynamic test, the acting force on the test specimen is applied exteriorly by loading actuator, which makes it unnecessary for the real quality on the test specimen to produce the inertial force. Hence, a virtual mass is the model quality worked out by the dynamic similar relations. It is enough to input the model quality as the numerical value in the initial conditions of the pseudo-dynamic test and there is no need to apply the quality on the test specimen (Fan *et al*. 2006). But meanwhile, the test specimen must meet the similar condition of the vertical load and as for the bracing piece; the requirement that the axial compression ratio should be similar must be met. With numbers of layers and low requirement in the quality of the vertical load, the model adopts the approach of placing counterweight on the floor surface to fix the mass block and then to attach the vertical load. Compared with the approach of vertical anchor or gantry with jack, this approach can make sure that there is no change of the size and orientation of the vertical load so that it can be avoided that the vertical load's direction is not stable. Due to the deformation of the test specimen, the earth anchor will incline to produce the horizontal components and additional stiffness is formed on the whole structure and effect will be brought to the structure's real restoring force.

Therefore, in order to satisfy the quality of the model and prototype and the similarity relation (JGJ101-96 1997), by using the additional mass technique, the counterweights like weights are uniformly applied on the floor for each layer. Table 3 is the result of the calculation with a 1/4 scaled specimen. Given that the purpose of the test is to study the effect of stiffness of the plate on the seismic performance of the whole structure. Therefore, it is inappropriate for the plate to produce larger defection in the vertical direction and as a result, the approach of less weight loaded is used to adjust the appropriate coefficient and eventually the vertical load of 1500 kg is evenly applied to each floor.

2.4.3 Monitoring point arrangement

To collect the data of the strain and deformation, resistance strain gauges are symmetrically arranged on the key parts such as the steel column, shear wall, the bottom brace and so on. In order to measure the floor's horizontal displacement, the displacement meters are arranged at the beam-column joints of each layer and the centre of long span plate. Meanwhile, the MTS' magnetic displacement sensor is arranged at the loading plate with 130 measuring points laid out on the strain gauge and 15 on the displacement meter. All the data of measuring points are collected, recorded and processed by the intelligent signal analyzer collection and processing. Fig. 6 is the vertical view of the model's displacement meter's arrangement and Fig. 7 shows the experiment device of the structural model. The setup for the testing schedule is shown in Fig. 7.

2.4.4 Selection of seismic wave

Code for Seismic Design of Buildings (GB50011 2010) requires that a group of EL Centro waves and Taft waves should be used as the seismic wave in this pseudo dynamic test. To observe

Table 3 The test model's weight (Units: kg)

Layer	Prototype mass	The model mass	Weight	Steel bearing mass
1	18096	484	647	897
2	19401	498	715	
3	19401	498	715	
total	56898	1480	3556	

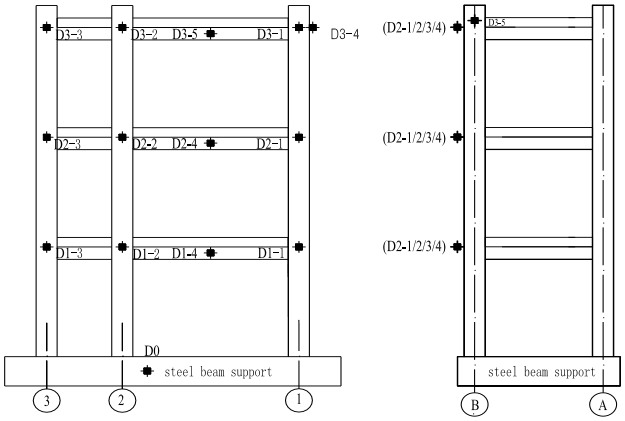

Fig. 6 Elevation layout of the displacement meter arrangement

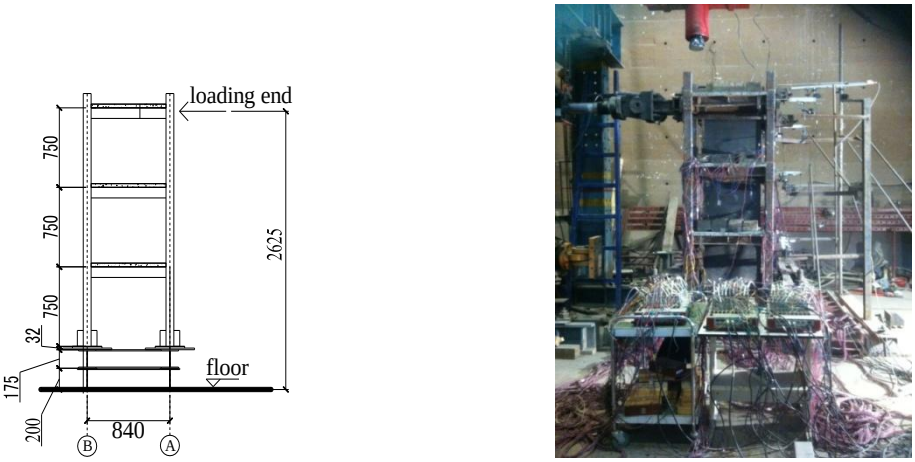

Fig. 7 Test set-up of the frame-shear wall structure (Units: mm)

the features of the seismic response that the model shows under different earthquake intensity, the sequence of the excitation conditions is designed into the earthquake intensity with the equation of 7-degree basic, severe and 8-degree, 9 degree severe. According to the principle of the seismic wave's certainty of duration and original records, the seismic wave's duration is 17.64 s, Δt = 0.01s. The total sample is 1,000 steps, of which forced period is 800 steps and free vibration period is 200 steps.

3. Process and phenomenon of the test

There is almost no crack appearing on the test specimen under the influence of EL Centro (NS) wave and Taft wave and with an acceleration of 100 gal. Under EL Centro (NS) wave and Taft wave and with an acceleration of 200 gal, along the direction paralleling to the long axis, a small number of subtle and none penetrating longitudinal cracks appear on the floor's side of each layer. Under EL Centro (NS) wave and with an acceleration of 400 gal, shear deformation happens to the steel plates shear wall and meanwhile, the wall clunks. At the bottom of each long span floors appear subtle and none penetrating cracks and parts of the plates have some longitudinal cracks through .Under EL Centro (NS) wave and with a peak acceleration of 620 gal, the cracks in the plate bottom slightly crack at a 45-degree angle and the sides of the longitudinal cracks

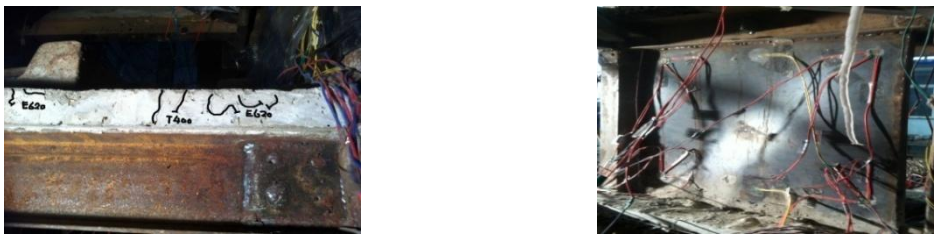

(a) Floor crack (b) Shear-wall tension field

Fig. 8 The damage of test specimens

continuously increase. The concrete on the edge of the second floor slightly flakes away and the shear wall of the second and third floor cambers. It is observed that cross-tension belt is clearly formed and the wall clunks loudly. After the test is finished, there is no obvious crack for the whole structure except that part of the steel plate shear wall's buckling and the whole structure doesn't go into the plastic stage. The damage of the test specimen is shown in Figs. 8(a)-(b).

4. Results and discussions

4.1 Displacement reaction

By processing the data gained by collecting the displacement meter of D1-3, D2-3 and D3-3 (Chen et al. 2004), the roof displacement-time curve of the test specimen can be seen in Figs. 9(a)-(b) under EL Centro (NS) wave and with the peak acceleration of 400 gal and 620 gal; under the influence of four different operating mode, EL Centro (NS) wave and Taft wave, its displacement envelope are shown in Figs. 10(a)-(b).

From Fig. 10(a), the roof displacement of each layer increases with the acceleration of input peak. Under EL Centro (NS) wave and with the acceleration of 100 gal and 200 gal, the displace-

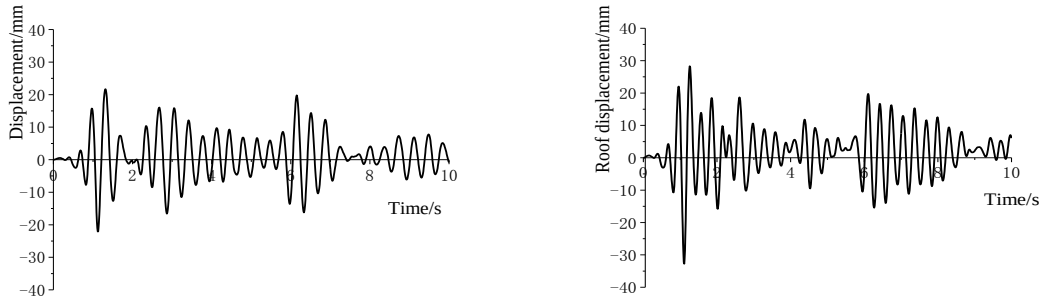

(a) Roof displacement time history curve of El Centro (NS) 400gal

(b) Roof displacement time history curve of El Centro (NS) 620gal

Fig. 9 The roof displacement-time history curve

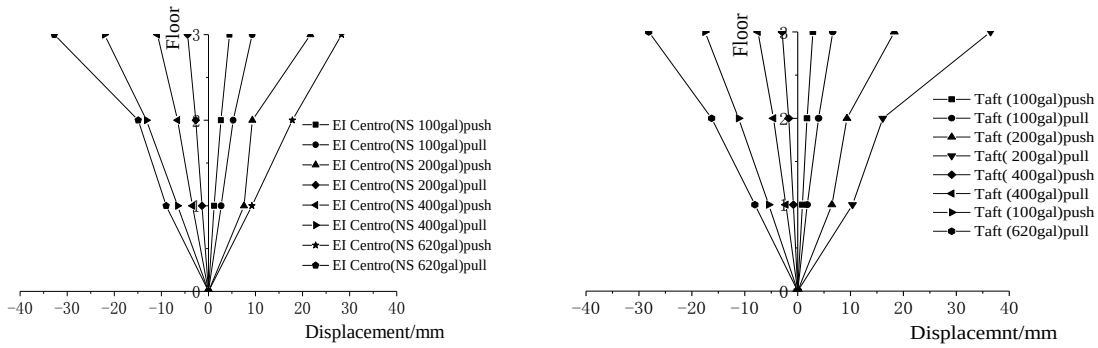

(a) El Centro (NS) wave

(b) Taft wave

Fig. 10 Displacement envelope

ment of one to three layers evenly changes and the reaction peak of the displacement is small. Under EL Centro (NS) wave and with the acceleration peak of 400 gal and 620 gal, the displacement of the second and third layers has the phenomenon of sudden increase and with the same working operating mode, bigger deviation appears in the direction of the actuator's pushing and pulling, which shows that with the model's accumulation of damage, the structural model has plastic nature to some extent. Through the analysis of the experimental phenomenon, the reason is that the buckling of the steel plate shear wall causes the decrease of the test specimen's whole stiffness and farther more, results in the sudden increase of the displacement. In different working conditions, Taft wave has the same trend and reason with EL Centro (NS).

4.2 Hysteresis loops and energy dissipation

In the pseudo-dynamic test, because of the restriction of the model's low floor height, there is no way to realize the two actuators' being installed in place at the same time, so the study is carried out with the 3-story model being the equivalent of single freedom system and meanwhile, the loading point of the actuator is fixed at the node of the second axis between the third floor's column and girder. Suppose: (1) multi-degree of freedom system produces seismic response according to assumed lateral shape; (2) multi-degree of freedom system is equal to the base shear of the equivalent single degree of freedom system; (3) the work is equal that horizontal seismic force makes in two systems.

By formula derivation based on the assumption (Medhekar and Kennedy 2000, Priestley *et al*. 2007, Liang 2011), the following is the result.

$$u_{eff} = \frac{u_r}{r_1} \tag{1}$$

$$r_1 = \frac{\sum_{i=1}^{n} m_i \phi_{1i}}{\sum_{i=1}^{n} m_i \phi_{1i}^2} f_y \tag{2}$$

In the Eqs.(1)-(2), u_{eff} is the equivalent displacement; u_r is the top displacement of multi-degree of formula; r_1 is the modal participation factors of the first mode of vibration; m_i is the quality of the structure's i floor; ϕ_{1i} is the modal value of the i particle of the first mode of vibration.

It is deduced from the above that if the top displacement of the original system of the multi-degree of freedom is known, the equivalent displacement of an effective single-degree-of- freedom system can be determined. Hence, based on the top displacement of the original system of the multi-degree of freedom, the equivalent displacement of an effective single-degree-of-freedom system can be determined and by corresponding to the restoring-force, the hysteresis loop of the equivalent displacement of an effective single-degree-of-freedom system can be constructed (Newcombe *et al*. 2010), as is shown in the Figs. 11(a)-(d).

Under EL Centro (NS) wave and with an acceleration of 100 gal and 200 gal, the lateral displacement is very small and there is a linear relationship between the load and displacement. With the increase of input acceleration peak value, the area of Hysteresis loops obviously becomes larger and the energy-dissipating capacity increases. Under EL Centro (NS) wave and with an acceleration of 400 gal, an apparent pinching phenomenon appears on the Hysteresis loops. From

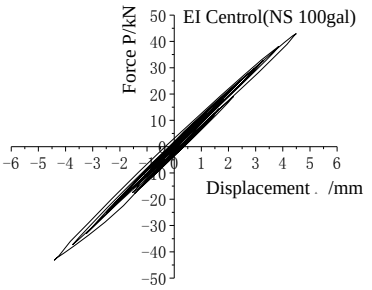

(a) Lateral load-displacement hysteresis loops

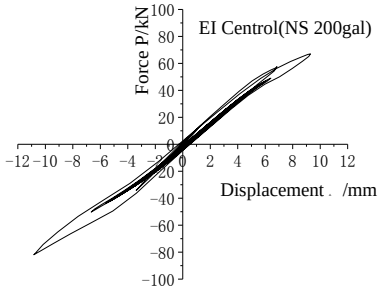

(b) Lateral load-displacement hysteresis loops

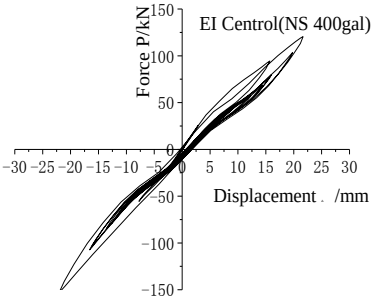

(c) Lateral load-displacement hysteresis loops

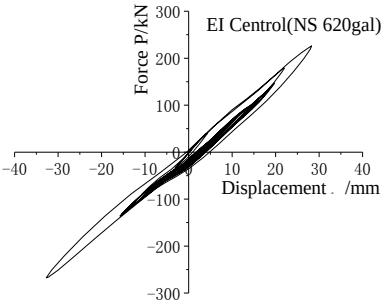

(d) Lateral load-displacement hysteresis loops

Fig. 11 Hysteresis loops of equivalent top force -displacement

that in the steel frame-shear wall system, the shear wall structure plays a leading role during the initial period and bears the horizontal load. With the increase of load and displacement, the stiffness of the shear wall decreases and thus the pinching phenomenon appears. Under EL Centro (NS) wave and with an acceleration of 600 gal, the hysteresis loops continues to increase, which shows that the ability to absorb energy is still increasing. The hysteresis under different working conditions curve plumps and with the increase of the peak acceleration, the area of the hysteresis loops continuously increases, which shows that the structure has good energy-dissipating capacity.

4.3 Deformation performance

During the process of the pseudo-dynamic, by collecting the displacement data of each measure point with the displacement meter and the data processed, the inter-laminar maximal displacement and maximal displacement angle for the structure model is obtained .They are shown in Tables 4-5.

It is seen from the Tables' 4-5 that under the influence of the same working condition of two types of seismic wave, all the elastic inter-story drift angle between the layers don't exceed the limits of 1/250 about the multi-story and high buildings steel structure elastic inter-story drift angle in code for seismic design of building (GB50011 2010) and satisfy the demand of undamaged under minor earthquake in seven- degree area; under nine-degree severe earthquake, the maximal inter-story drift angle of the test specimen can reach under different working conditions is 1/42 and1/37, which all exceed the elastic-plastic inter-story drift angel limit 1/50, while the whole structure is in good condition, meeting the demand of no collapse under strong earthquake, and showing that the fabricated structure has good anti-seismic performance.

Table 4 The inter-story drift and inter-story drift angle under El Centro (NS) wave

Working condition	Loading story	Inter-story drift /mm		Inter-story drift angle	
		Activator push	Activator pull	Activator push	Activator pull
100 gal	1	1.22	1.35	1/615	1/556
	2	1.44	1.33	1/521	1/564
	3	1.83	1.73	1/410	1/434
200 gal	1	2.72	3.41	1/276	1/220
	2	2.54	3.12	1/295	1/240
	3	4.04	4.31	1/186	1/174
400 gal	1	7.57	6.54	1/99	1/115
	2	1.77	6.61	1/424	1/114
	3	12.33	8.91	1/61	1/84
620 gal	1	9.25	8.98	1/81	1/84
	2	8.59	5.91	1/87	1/127
	3	10.45	17.84	1/72	1/42

Table 5 Inter-story drift and inter-story drift angle under Taft wave

Working condition	Loading story	Inter-story drift /mm		Inter-story drift angle	
		Activator push	Activator pull	Activator push	Activator pull
100 gal	1	0.87	0.79	1/862	1/949
	2	0.9	0.91	1/833	1/824
	3	1.13	1.21	1/664	1/620
200 gal	1	1.8	2.23	1/417	1/336
	2	2.18	2.35	1/344	1/319
	3	2.64	2.91	1/284	1/258
400 gal	1	6.48	5.47	1/116	1/137
	2	2.86	5.69	1/262	1/132
	3	8.94	6.34	1/84	1/118
620 gal	1	10.37	8.07	1/72	1/93
	2	5.73	8.17	1/131	1/92
	3	20.36	11.91	1/37	1/63

4.4 Inter-story drift stiffness

In order to learn the stiffness degradation rule, choose the loading's sum of the absolute value in the positive and negative directions under repeated loading to divide the sum of the absolute value of the corresponding displacement and then get the average stiffness of circulation for each level K_i (Xue *et al*. 2014)

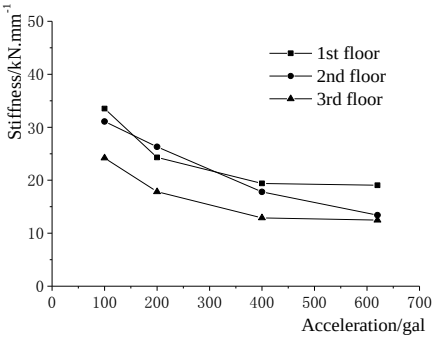

(a) Inter-story stiffness under El Centro (NS) wave

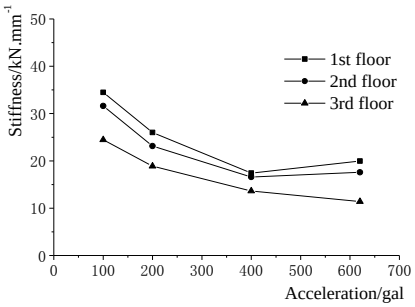

(b) Inter-story stiffness under Taft wave

Fig. 12 Curves of stiffness degradation

$$K_i = \frac{|P_i|+|-P_i|}{|\Delta_i|+|-\Delta_i|} \tag{3}$$

In the Eq. (3), P_i and Δ_i are the maximum loading value reached by loading the i time and corresponding displacement value.

According to the experimental data, and under EL Centro (NS) wave and Taft wave, the average stiffness of the inter-story can be Fig. 12 out, and Figs. 6-7 show the result. By the statistics of the average stiffness changes for each layer, stiffness degradation curve between the layers can be got, which can be seen in Figs. 12(a)-(b). By comparing and analyzing the average stiffness changes, under the seismic load, the specimen stiffness constantly declines with the damage calcu1ation and the total trend is steady.

Table 6 Inter-story shear of test specimen and average stiffness under El Centro (NS) wave

Working condition	Loading story	Inter-story shear /kN		Average stiffness kN/mm
		Activator push	Activator pull	
100 gal	1	42.96	43.17	33.51
	2	42.96	43.17	16.13
	3	42.96	43.17	9.68
200 gal	1	67.03	81.88	24.29
	2	67.03	81.88	12.63
	3	67.03	81.88	7.39
400 gal	1	120.48	153.25	19.4
	2	120.48	153.25	12.17
	3	120.48	153.25	6.26
620 gal	1	226.19	267.56	27.08
	2	226.19	267.56	15.09
	3	226.19	267.56	8.09

Table 7 Inter-story shear of test specimen and average stiffness under Taft wave

Working condition	Loading story	Inter-story shear /kN		Average stiffness kN/mm
		Activator push	Activator pull	
100 gal	1	28.24	29	34.48
	2	28.24	29	16.5
	3	28.24	29	9.85
200 gal	1	51.35	53.44	23.5
	2	51.35	53.44	12.24
	3	51.35	53.44	7.43
400 gal	1	97.85	110.35	17.42
	2	97.85	110.35	10.16
	3	97.85	110.35	5.82
620 gal	1	185.98	181.87	19.95
	2	185.98	181.87	11.37
	3	185.98	181.87	5.69

5. Conclusions

By studying pseudo-dynamic test of the steel frame - shear wall with prefabricated floor structure, the indexes of the structure's displacement response, energy dissipation, overall deformation and stiffness degradation can be derived and the conclusions are as follows:

- The steel frame - shear wall with prefabricated floor structure is of good deformation performance. The residual deformation is small after unloading.
- When the model is in the elastic stage, the inter-story displacements are satisfactory with the limit regulations in code for seismic design of building (GB50011 2010) for the high-rise steel structure elastic story-drift that the maximum inter-story drift angle is $[\theta_e]$ = 1/250, and under rarely occurred 9-degree earthquake, the maximum inter-story drift displacement angle is 1/37 which exceeds the limit that the high-rise steel structure elastic-plastic inter-story drift angle is $[\theta_p]$ = 1/50. After the test, buckling only happens to the steel plate shear wall, while there are no obvious cracks on the frame column and floor diaphragm and they are in good condition. It is proved that the structure's fortification objects meet the requirement of "no damage after mild earthquake, little damage while moderate earthquake, no collapse after severe earthquake".
- During the whole test, obvious cracks don't appear, especially at the joints between the precast floor diaphragms, precast floor diaphragms and girders, and at the bracing of plate bottom girder. All these phenomena demonstrate that the new connection method and the way to arrange horizontal bracing at the bottom of plate can effectively improve the integrity of precast floor diaphragms. Therefore, the technique can be adopted in areas with high seismic intensity.

Acknowledgments

The authors would like to thank the Innovation The local science and technology project of

Hebei Province (Grant No. 2011188) and Xi'an University of Architecture and Technology for their generous support of this research work.

References

Chen, C.H., Hsiao, P.C., Lai, J.W., Lin, M.L., Weng, Y.T. and Tsai, K.C. (2004), "Pseudo-dynamic test of a full-scale CFT/BRB frame: Part 2—Construction and testing", *Proceedings of 13th World Conference on Earthquake Engineering*, Vancouver, BC, Canada, August, Paper No. 2175.

Chen, Z.X., Xu, G.S., Wu, B., Sun, Y.T., Wang, H.D. and Wang, F.L. (2014), "Equivalent force control method for substructure pseudo-dynamic test of a full-scale masonry structure", *Earthq. Eng. Struct.*, **43**(7), 969-983.

Fan, L., Zhao, B. and Lu, X.L. (2006), "Discussion on some problems in pseudodynam ic tests", *Struct. Engrs.*, **22**(5), 50-53.

Fan, Y.L., Guo, Y.R., Xiao, Y., Li, F.W. and Shan, B. (2007), "Development in remote collaborative pseudo-dynamic testing platform for single story structures", *J. Earthq. Eng. Eng. Vib.*, **27**(3), 77-82.

Fleischman, R., Restrepo, J., Naito, C., Sause, R., Zhang, D. and Schoettler, M. (2012), "Integrated analytical and experimental research to develop a new seismic design methodology for precast concrete diaphragms", *J. Struct. Eng.*, **139**(7), 1192-1204.

GB50011 (2010), *Code for Seismic Design of Buildings*, China Architecture & Building Press, Beijing, China.

JGJ101-96 (1997), *Specificating of Testing Methods for Earthquake Resistant Building*, China Architecture & Building Press, Beijing, China.

Li, Q.N., Chen, M.G. and Jiang, W.S. (2014), "Shaking table test study on a new assembled monolithic floor-steelplate and frame shear wall structure", *Sichuan Build. Sci.*, **40**(2), 158-163.

Liang, X.W. (2011), *The Design Theory and Method of Structural Seismic Performance*, Science Press, Beijing, China.

Lu, T.J., Qin, S.J., Luo, Y.S. and Yu, Z.W. (2009), "Pseudo-dynamic experimental study on high rise steel-concrete hybrid structure", *J. Build. Struct.*, **30**(3), 27-35.

Medhekar, M. and Kennedy, D. (2000), "Displacement-based seismic design of buildings—theory", *Eng. Struct.*, **22**(3), 201-209.

Nakashima, M., Kato, H., Takaoka, E., Nakashima, M., Kato, H. and Takaoka, E. (1992), "Development of real-time pseudo dynamic testing", *Earthq. Eng. Struct.*, **21**(1), 79-92.

Nakashima, M., Akazawa, T. and Igarashi, H. (1995), "Pseudo-dynamic testing using conventional testing devices", *Earthq. Eng. Struct.*, **24**(10), 1409-1422.

Newcombe, M.P., van Beerschoten, W.A., Carradine, D., Pampanin, S. and Buchanan, A.H. (2010), "In-plane experimental testing of timber-concrete composite floor diaphragms", *J. Struct. Eng.*, **136**(11), 1461-1468.

Paquette, J. and Bruneau, M. (2003), "Pseudo-dynamic testing of unreinforced masony building with flexible diaphragm", *J. Struct. Eng.*, **129**(6), 708-716.

Paquette, J. and Bruneau, M. (2006), "Pseudo-dynamic testing of unreinforced masonry building with flexible diaphragm and comparison with existing procedures", *Construct. Build. Mater.*, **20**(4), 220-228.

Priestley, M., Calvi, G. and Kowalsky, M. (2007), "Direct displacement-based seismic design of structures", *2007 NZSEE Conference*.

Ren, R. and Naito, C. (2012), "Precast concrete diaphragm connector performance database", *J. Struct. Eng.*, **139**(1), 15-27.

Shi, Q.X., Wang, S.L., Su, S.Q., Wang, Q.W. and Zhu, J.Q. (2011), "Pseudo-dynamic test of a reinforced concrete frame-shear wall model structure", *China Civil Eng. J.*, **44**(7), 1-9.

Sun, G.X., Ma, X.R., Zhang, W.Q. and Sun, L. (2010), "Constructing assembled type residence pushes forward industrialization of residential construction", *Hous. Sci.*, **12**, 34-37.

Wu, B., Xu, G., Li, Y., Shing, P.B. and Ou, J. (2012), "Performance and application of equivalent force control method for real-time substructure testing", *J. Eng. Mech. - ASCE*, **138**(11), 1303-1316.

Xue, J.Y., Gao, L., Liu, Z.Q., Zhao, H.T. and Chen, Z.P. (2014), "Experimental study on mechanical performances of lattice steel reinforced concrete inner frame with irregular section columns", *Steel Compos. Struct., Int. J.*, **16**(3), 253-267.

Zhang, D., Fleischman, R., Naito, C. and Ren, R. (2010), "Experimental evaluation of pretopped precast diaphragm critical flexure joint under seismic demands", *J. Struct. Eng.*, **137**(10), 1063-1074.

Zheng, X.C., Li, Q.N., Pan, S.B. and Jiang, W.S. (2013), "The shaking table test on a prefabricated integral frame-shear wall structure with a new prefabricated floor", *J. Earthq. Eng. Eng. Vib.*, **33**(3), 141-142.

BU